ECOS 2016: Numerical model of an externally fired gas turbine, including an arbitrary number of stages in expansion and compression processes

Álvaro Durante[a,1], Gabriel Pena-Vergara[a,2], Pedro Curto-Risso[a,3],Alejandro Medina[b,4], and Antonio Calvo Hernández[b,5]

[a]*Universidad de la República, DepartmentofAppliedThermodynamics, Montevideo, Uruguay.*
[b]*Universidad de Salamanca, DepartmentofAppliedPhysics, Salamanca, Spain.*
[1]adurante@fing.edu.uy; [2]gabpena@fing.edu.uy; [3]pcurto@fing.edu.uy
[4]amd385@usal.es; [5]anca@usal.es

Abstract:

A thermodynamic model for a realistic Brayton cycle, working as an externally-fired gas turbine, fueled with biomass, is presented. The use of an external combustion chamber, allows to burn “dirty fuels” to preheat pure air, which is the turbine's working fluid. It also avoids direct contact of ashes with the turbine blades, resulting in a higher life cycle of the turbine. Due to the high temperatures achieved by the combustion gases, high temperature heat exchangers (HTHE) will be needed. The model incorporates a HTHE and an arbitrary number of turbines and compressors, with the corresponding number of inter-coolers and re-heaters. It considers irreversibilities such as non-isentropic processes and pressure losses. The composition and temperature of the combustion gases, as well as the variable flow rate of air and combustion gases, are calculated for an specific composition of the fuel. The numerical model has been validated according to the AE-T100E Micro Turbine Externally Fired data sheet, fueled with natural gas and a single stage cycle. The power of 85kWe and electrical efficiency of 24% is obtained. In addition we perform a comparative validation with a directly fired gas turbine, Turbec T100, working at the same conditions and the results are good agreement considering the similarity of the technologies.

Keywords:

Brayton cycle, Externally fired gas turbine, Solid fuels

1. Introduction

From an environmental perspective, the sustainability of development depends, among other measures, on the reduction of greenhouse gas emissions and the conservation of soil and water. This requires a rational use of fossil fuels and the utilization of renewable natural resources. Among human activities, the energy production is one of the most intensively demanding natural resources. On the other hand, it is also the biggest source of pollutants emissions [1]. The future world energy-supply will have to rely on all energy resources, especially renewable energies. Future technologies should combine high conversion-efficiencies with low emissions, in particular CO_2 and other greenhouse gases [2]. Biomass is getting more attention as a renewable energy source because of its potential to reduce greenhouse emissions supplying fossil sources. However, for large scale power plants, it is not always possible to consider biomass as an affordable fuel since processing costs are high [3]. Because of that, some power plants projects are economically unviable.

Some of the energy-conversion technologies, like internal-combustion engines and gas turbines, need clean fuels as the combustion gases are in direct contact with the moving parts of the machine. Indirect systems separate the combustion and the thermodynamic conversion cycle. The Rankine cycle, which could be operated with solid fuels such as coal or biomass, is the best example. The same principle applies to the Stirling engine. The indirectly or externally-fired gas-turbine (EFGT) is other technology under development for small and medium scale power-and-heat supplies [2].

Since the turbine working fluid is separated from the combustion gases, the thermal power of the combustion gases should be transferred to the working fluid via a high temperature heat exchanger (HTHE). Unlike the directly fired gas turbine (DFGT), EFGTs can work on an open cycle with air as the working fluid, or a closed cycle with air or other fluid having better thermodynamic properties [4]. DFGT can deal only with clean fuels. It can also deal with solid fuels like coal and biomass but only after a gasification process with an intensive gas cleaning process. EFGTs can deal with a wide range of fuels even solid fuels without cleaning systems or fuel compression and injection equipments. It is very flexible and can use a wide range of thermal power sources such as combustors, furnaces, solar power concentrators, and even nuclear reactors [4]. The net efficiency of EFGTs can be improved in combined heat and power systems.
The aim of the present work is to simulate an externally fired gas turbine from a thermodynamic viewpoint and to analyze how the net power and cycle efficiency are affected by considering different compositions of biomass fuels and multi-stage compression and expansion processes. The model incorporates a ceramic heat exchanger and an arbitrary number of turbines and compressors, with the corresponding number of intercoolers and pre-heaters (or burners).

2. Theoretical Model

The model studied consists of an arbitrary number of N_t turbines and N_c compressors, with the corresponding $(N_c - 1)$ intercoolers and $(N_t - 1)$ intermediate burners (see Fig. 1). The ideal cycle (see Fig. 2) can be summarized as follows: the air, as working fluid, at pressure, P_1, and temperature, T_1, is compressed, by N_c adiabatic compressors, to pressure, P_2, and temperature, T_2; then increases its temperature up toT_3 in an isobaric ceramic heat exchanger (HTHE). This air is expanded, by N_t adiabatic turbines, to a pressure and temperature, P_4 and T_4, respectively. Next, the air is used to supply the combustion chamber to burn a solid fuel. The exhaust gases are used as the hot fluid in the HTHE at temperature, T_{ad}, then are released to the ambient at T_{ch}. Between each compression process, heat is extracted by the intercooler in order to decrease the temperature, at each compressor inlet, to T_1. In the same manner, between each expansion process, heat is supplied by the intermediate burners in order to increase the temperature, at each turbine inlet, to T_3. The burned gases are released to the ambient at temperature T_{e2}.

All compressors are considered to have the same pressure ratio r_c as well as the turbines, with a pressure ratio r_t. The turbines inlet temperature, T_3, is fixed according to a constructive and metallurgical limit. In the main combustion chamber the biomass is burned with clean air out coming from the last turbine at temperature T_4. The equivalence ratio, ϕ_1, of this combustion is calculated so that the adiabatic flame temperature T_{ad} obtained allows to reach T_3 at the exit of the ceramic high temperature heat exchanger (HTHE) [5,6]. The combustion in the burners, which allows to heat the clean air from T_3 to T_4 in a separate circuit, uses air from the ambient at T_1. The equivalence ratio of this combustion, ϕ_2, is calculated so that the adiabatic flame temperature obtained matches with the one reached in the main combustion chamber. This procedure ensures that the heat exchange is physically possible and allows setting a pinch point of 100K, on the exhaust gases temperature T_{e2} as construction criteria.

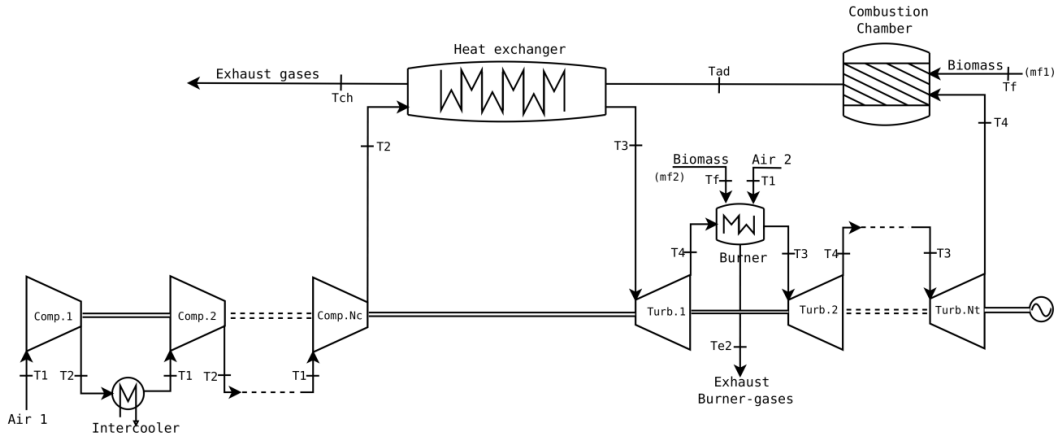

Fig. 1. Scheme of a multi-stage externally fired gas turbine, with burners between expansion processes and intercoolers between compression processes.

The present work attempts to reproduce realistic performance records for an EFGT starting from the ideal model and introducing the main irreversibilities existing in real plants as pressure drops, non-ideal heat exchangers, and isentropic efficiencies in compressors and turbines.

2.1. Thermodynamic model

The thermodynamic model of a multi-step Brayton cycle is based on those presented by Sánchez-Orgaz et al. [7,8] and Roco et al. [9]. The present work adapts the numerical model of [10] for the use of an external biomass-fuelled combustion chamber, taking into account the chemical reactions in the combustion of solid fuels. Fig. 2 represents the thermodynamic cycle, considering pressure drops and irreversibilities in compression and expansion processes, that are considered as non-adiabatic. Next we detail the main assumptions and definitions for each stage.

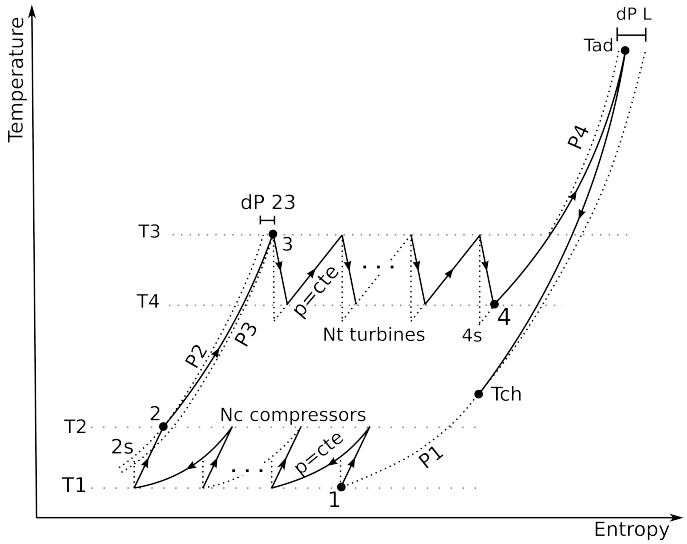

Fig. 2. Temperature-entropy diagram for a multi-stage externally fired Brayton cycle.

2.1.1. Compression and expansion

Defining the pressure ratio of a compressor as, $r_c = ({p_2}^i/{p_1}^i)$, where ${p_1}^i$ and ${p_2}^i$ are the inlet and outlet pressures of the *i*th compressor respectively, considering N_c compressors with the same value of r_c, P_1 as the inlet pressure of the first compressor (assumed in this work as atmospheric pressure) and P_2 the outlet pressure of the last compressor (see Fig. 2), it is easily proven that

$$P_2 = P_1\, r_c^{Nc} \qquad (1)$$

Since the ideal compression process is isentropic, and considering $\bar{\gamma}_1$ as the mean isentropic coefficient between 1 and 2s (see Fig. 2), we define the isentropic compressor pressure ratio,

$$a_c = \frac{T_{2s}}{T_1} = r_c^{\frac{\bar{\gamma}_1 - 1}{\bar{\gamma}_1}} \quad (2)$$

In order to take into account the compression irreversibilities, the isentropic efficiency is defined as

$$\varepsilon_c = \frac{T_{2s} - T_1}{T_2 - T_1} \quad (3)$$

With equations (2) and (3) it is possible to obtain [7];

$$\frac{T_2}{T_1} = Z_c = 1 + \frac{a_c - 1}{\varepsilon_c} \quad (4)$$

where Z_c is defined for convenience. The pressure ratio of one turbine,r_t, is calculated using N_t, P_2, and all the pressure losses in the circuit.The pressure drop in the cold side of the heat exchanger is denoted as dP_{23}, and the pressure drop in the hot side of the heat exchanger is dP_L. Considering the intercoolers and re-heaters (intermediate burners) as isobaric, the global pressure ratio for the N_t turbines is calculated as

$$r_{t_G} = \frac{P_3}{P_4} = \frac{P_2 - dP_{23}}{P_1 + dP_L} \quad (5)$$

where P_3 is the pressure at the inlet of the first turbine and P_4 is the pressure at the outlet of the last one. Proceeding in the same way as for (1), the pressure ratio of one turbine is,

$$r_t = \left(r_{t_G}\right)^{1/N_t}. \quad (6)$$

In the same way as for compression, the isentropic turbine pressure ratio is:

$$a_t = \frac{T_3}{T_{4s}} = r_t^{\frac{\bar{\gamma}_2 - 1}{\bar{\gamma}_2}}, \quad (7)$$

The following parameters and equations allow to connect temperatures with the turbine pressure ratio:

$$\varepsilon_t = \frac{T_3 - T_4}{T_3 - T_{4s}}, \quad (8)$$

$$\frac{T_4}{T_3} = Z_t = 1 - \varepsilon_t(1 - a_t^{-1}). \quad (9)$$

where $\bar{\gamma}_2$ is the mean isentropic coefficient of air among the state 3 and 4 (see Fig. 2), and $\varepsilon_t$is the isentropic efficiency of the turbines considered identical.

2.1.2. Heat input

Since the system is externally fired, the process of heat addition to the working fluid is performed by a ceramic heat exchanger between burned gases, coming from a combustion chamber, and the working fluid. To solve all temperatures of heat exchanger we use a NTU method (see Section 2.2) and energy balance on the heat exchanger,

$$\dot{m}_{a,1}[h_a(T_3) - h_a(T_2)] = \dot{m}_{g,1}\left[h_{g,1}(T_{ad}) - h_{g,1}(T_{ch})\right], \quad (10)$$

where, $\dot{m}_{a,1}$ is the air mass flow in the compression process, h_a and $h_{g,1}$, the enthalpy of air and combustion gases, from combustion chamber, respectively, at the temperatures mentioned (see Fig. 2), T_{ad}, the adiabatic flame temperature, T_{ch}, the exhaust temperature, and $\dot{m}_{g,1}$, the mass flow rate of burned gases. The value of $\dot{m}_{g,1}$ is obtained by a mass balance for the combustion chamber:

$$\dot{m}_{g,1} = \dot{m}_{f,1} + \dot{m}_{a,1} \quad (11)$$

where $\dot{m}_{f,1}$is the fuel mass flow. After obtainingT_{ad}, it is easy to determine the equivalence ratio to reach this temperature, solving the combustion process and burned gases composition (see Secs. 2.3. and 2.4.).

Other heat inputs come from the intermediate burners. Again, using NTU method and energy balance and the hypothesis of pinch point (mentioned at the beginning of section 2), it is possibly to determine the exhaust temperature, the secondary flow mass, $\dot{m}_{f,2}$, and equivalence ratio of the burners, ϕ_2.

$$\dot{m}_{a,1}[h_a(T_3) - h_a(T_4)] = \dot{m}_{f,2}.h_f(T_f) + \dot{m}_{a,2}h_a(T_1) - \dot{m}_{g,2}h_{g,2}(T_{e2}) \quad (12)$$

where the subscript *2* denotes properties at the burners hot side. It is important to notice that the composition of the exhaust burners gases is different from the one calculated in the main combustion chamber.

2.1.3. Power and efficiency

With all temperatures of the cycle and main mass flow air, it is possible to calculate its net power by,

$$P = N_t\dot{m}_{a,1}[\,h_a(T_3) - h_a(T_4)] - N_c\dot{m}_{a,1}[\,h_a(T_2) - h_a(T_1)] \quad (13)$$

In order to take into account the quality of conversion energy in the system we consider the fuel conversion efficiency, that relates the heating value and usable energy of the thermal engine. It expression for time rates is:

$$\eta = \frac{P}{\dot{m}_f\, LHV} \quad (14)$$

Where LHV, is the lower heating value of the biomass and $\dot{m}_f$ is the total fuel rate that enters to the system. The mass, $\dot{m}_f$, is simply obtained by adding$\dot{m}_{f,1}$ and $\dot{m}_{f,2}$

$$\dot{m}_f = \dot{m}_{f,1} + \dot{m}_{f,2} \quad (15)$$

where$\dot{m}_{f,1}$ is obtained with the knowledge of the value of the equivalence ratio ϕ_1 and $\dot{m}_{f,2}$, directly by solving chemical reactions at the intermediate burners.

2.2. Heat Exchangers

To evaluate the performance of the heat exchanger it is necessary to introduce its effectiveness, ε, which varies according to the working conditions, such as mass flow rates, fluids properties and temperatures, using the NTU method [11]. The effectiveness of the heat exchanger is defined as (see Fig. 2 for the temperatures),

$$\varepsilon = \frac{T_3 - T_2}{T_{ad} - T_2}, \quad (16)$$

For any heat exchanger it is shown [11] that $\varepsilon = f(NTU, C_r)$, considering the *number of transfer units*, *NTU*, as

$$NTU = \frac{UA}{C_{min}} \quad (17)$$

where UA is the global exchange coefficient of the heat exchanger, C_{min} the minimum heat capacity rate and $C_r = \frac{C_{min}}{C_{max}}$ heat capacity ratio .

We make use of a counter-flow scheme to model the heat exchanger [6][11]

$$\varepsilon = \frac{1 - e^{-NTU\,(1 - C_r)}}{1 - C_r e^{-NTU\,(1 - C_r)}} \quad (18)$$

From the correlations of the *Nusselt* number for internal flow [11] and considering the hypothesis that the thermodynamic properties of the working fluids do not change considerably within the

range of temperatures taken into account, nor due to its composition, the convection coefficient for air and exhaust gases, are only affected for variations in the mass flow rate of any of the working. Therefore, NTU could be expressed by,

$$NTU = \frac{K}{C_{min}\left[(\dot{m}_a)^{-0.8}+(\dot{m}_g)^{-0.6}\right]} \qquad (21)$$

where the coefficient K depends on the geometry of the heat exchanger and thermodynamic properties of the working fluids. From the experimental work of Batista de Mello, et al. [6], the effectiveness of a ceramic high temperature heat exchanger can reach up to values of 0.84. In the present work the value of K is adjusted to reach this efficiency at same conditions.

2.3. Combustion Model

In order to solve the chemistry and the energetic of combustion we assume a certain wet fuel with a determined chemical composition and humidity. The considered chemical reaction is [12],

$$C_{\frac{a}{12}}H_{\frac{b}{1}}O_{\frac{c}{16}}N_{\frac{d}{14}} + fH_2O + \phi\alpha_q(O_2 + 3.76N_2) \longrightarrow \beta CO_2 + \gamma H_2O + \epsilon CO + \theta H_2 + \nu O_2 + \mu N_2 \quad (R1)$$

where a mole of dry fuel is represented by $C_{\frac{a}{12}}H_{\frac{b}{1}}O_{\frac{c}{16}}N_{\frac{d}{14}}$, with a, b, c, d the amount of each element in mass percentage. The coefficient f represents the moles of water per mole of dry fuel, ϕ the fuel-air equivalence ratio and α_q the stoichiometric amount of O_2 within the air, per mole of dry fuel. It is important to notice that this model does not consider the possible presence of sulfur in the fuel composition. The reason of this is that in spite that most of biomass fuels do have a percentage of sulfur in its compositions, in general it is not considerable. Particularly in this work the biomass fuels considered have less than 0.1% of sulfur. The combustion is solved following the procedure described by Medina et al. [13].

2.4. Adiabatic Flame Temperature

Once that the composition of burned gases is obtained, it is possible to calculate its enthalpy at a certain temperature T,

$$h_g(T) = x_{CO_2}.h_{CO_2}(T) + x_{H_2O}.h_{H_2O}(T) + x_{O_2}.h_{O_2}(T) + x_{N_2}.h_{N_2}(T) + x_{CO}.[h_{CO}(T) + LHV_{CO}] + x_{H_2}.\left[h_{H_2}(T) + LHV_{H2}\right] + x_{ash}.C_{p_{ash}}.\left(T - T_{ref}\right) \qquad (22)$$

where the coefficients x_i represents the moles of each compound per mass flow rate of combustion gasses, and LHV_j is the lower heating value at reference temperature, T_{ref}, of specie j.

The enthalpy of the fuel at a temperature T_f is,

$$h_{fuel} = c_{p,f}\left(T_f - T_{ref}\right) + LHV_f - f\left[h_{fg_{H_2O}} - C_{p_{H2Oliq}}.\left(T_{H_2O} - T_{ref}\right)\right] \qquad (23)$$

where it is assumed that the water present in the fuel is in liquid state and at the temperature of the fuel ($T_{H_2O} = T_f$).

The adiabatic flame temperature, T_{ad}, is defined as the temperature of the exhaust combustion gases when the combustion is considered adiabatic.This means that all the energy released during combustion is transferred to the exhaust gases without any heat losses. It is calculated through the thermodynamic balance (24), considering the air enthalpy as h_a,

$$\dot{m}_f h_f + \dot{m}_a h_a = \dot{m}_g h_g(T_{ad}) \qquad (24)$$

where the $\dot{m}_f$, $\dot{m}_a$ and $\dot{m}_g$ are the mass flows of fuel, air and burned gases respectively. The last one is obtained by a mass balance.

2.5. Validation

In order to validate the model we attempt to use the AE-T100E Micro Turbine Externally Fired data sheet single stage cycle, but is extremely dependent of inlet fuel, so the datasheet presents only values of pressure ratio, electrical power, air flow rate and inlet turbine temperature. With those data the model could reach the expected values, see Table 1.

Table 1 Values obtained from the model compared with EFGT AE-T100E

Parameter	AE-T100E	value	Relative error (%)
Fuel type	-	Methane	-
Gas-temperature turbine inlet	850ºC	850ºC	-
Mass flow air	0.80 kg/s	0.80 kg/s	-
Pressure ratio	4.5	4.5	-
Net electric - power output	85kW	86.3kW*	1.53
Net electric - efficiency	-	24%	-

*Considering an electric generator efficiency of 0.85

Since lack of data of EFGT, we compare quantitatively the performance of a similar DFGT Turbec T100. To reproduce the values of the Turbec T100, model parameters are set with those obtained from the data sheet, see Table 2.

Table 2 Model set values obtained from the data sheet of AE-T100E

Parameter	value
Fuel type	Methane
Gas-temperature turbine inlet	950ºC
Mass flow air	0.7833 kg/s
Pressure ratio	4.5
Efficiency compressor	0.768
Efficiency turbine	0.826

Considering an electric generator efficiency of 0.81, the Table 2 presents the results of our model, for one single stage and the values of the Turbec T100.

Table 3 Comparison of the model and values of Turbec T100

	Turbec T100	Present Model	Relative difference (%)
Net electric-output	100kW	98.82kW	1.18
Thermal-power input	333kW	360.68kW	8.31
Turbine power	282kW	281.34kW	0.23
Compressor power	159kW	158.37kW	0.40
Net electric-efficiency	30	0.276	8.00
Air temperature compressor outlet	214	214.4	0.18
Mass flow, natural-gas	0.0067	0.007188	7.28
Mass flow, exhaust-gas	0.79	0,7905	0.063

The values obtained by the model are in good agreement of those the Turbec T100. Is important to mention that the differences between the model and the turbine are not precisely due to numerical approaches, since we compare different technologies, but operating in the same conditions.

3. Numerical Results

This section uses the model presented in section 2 to analyze the development of an EFGT for different configurations, varying the number of compressors and turbines between one and two

units, using an intercooling and burner if necessary. Therefore we perform four configurations, described as next:

CT : One compressor and one turbine

CICT : Two compressors and intercooler, and one turbine

CTBT : One compressor, and two turbines and burner

CICTBT : Two compressors and intercooler, and two turbines and burner

Eucalyptus wood is used as the main fuel for the simulations. Other biomasses, such as pine wood, rice husk and eucalyptus forest residues were employed to study de influence of the elemental and ultimate compositions, as well as its lower heating value. All these characteristics are presented in the Table 4.

Table 4. Biomass elemental composition (d.b.), ash content (d.b.) and LHV.

Biomass	**C (%)**	**H (%)**	**O (%)**	**N (%)**	**Ash (%)**	**LHV (kJ/kg)**
Eucalyptus wood	49.0	5.9	44.0	0.3	0.1	18129
Eucalyptus leaves	54.9	5.9	35.8	1.0	2.4	19100
Eucalyptus bark	44.7	5.4	41.8	0.2	4.9	15800
Eucalyptus branches	52.9	5.9	39.9	0.2	1.2	18100
Eucalyptus tips	52.5	5.9	40.6	0.3	0.7	17900
Rice husk	41.0	5.9	35.9	0.4	18.9	14800
Pine wood	49.3	6.0	44.4	<0.01	0.3	18681

The ashes heat capacity was estimated using the Neumann-Kropp rule [11] and the ashes elemental composition for each one [12]. We find that the heat capacity for any of these biomasses is between 0.74 and 0.80 kJ/kg, so we decide to use 0.77 kJ/kg for all the samples.

3.1. Performance in function of the pressure ratio

The pressure ratio is one of the main design parameter that characterized the Brayton cycle performance. In this section we study the performance varying the pressure ratio in the range of 2 to 16. Eucalyptus biomass was employed as fuel, with 25% of moisture in dry basis. Other parameters of the simulation were the main air mass flow (1,0 kg/s), ambient temperature, T1 (300K), and turbine air inlet temperature, T3 (1173K).

Fig. 3 shows the net power achieved for each EFGT configuration. The highest power for each pressure ratio is obtained for CICTBT, followed by CTBT, CICT and CT in the last position. It can be seen, that the two configurations with two turbines get better net power. When the compression is made in two stages with intercooler, the net power increase compared to which ones the compression is made in one step. The net power curves show a maximum in the pressure rate studied, different for each one. This is an expected behavior of this kind of machines [7].

On the other hand, the efficiency behavior is different, where the EFGT configurations with one turbine are those which realize better results (see Fig. 4). Moreover, the fact that include the two stages compression improve the efficiency. Therefore, the fuel conversion efficiency decreases in the sequence CICT, CT, CICTBT, CTBT.

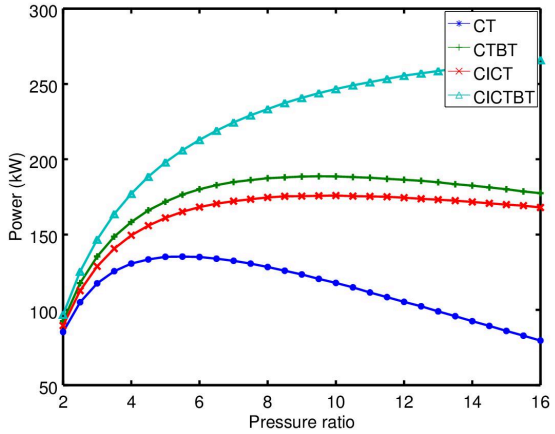

Fig. 3. Net power in function of the pressure ratio for different arrangement of compressors and turbines

The really big efficiency drop in two turbines configurations compared to these ones with one turbine is explained by the exhaust gases of the burner to reheat the air for the second stage of expansion. These gases leave the system at T_{e2}, which was setup 100ºC over T_4. Because of that, the amount of energy lose in the burners is very significant. In future works, that is an important point to improve in order to achieve best results.

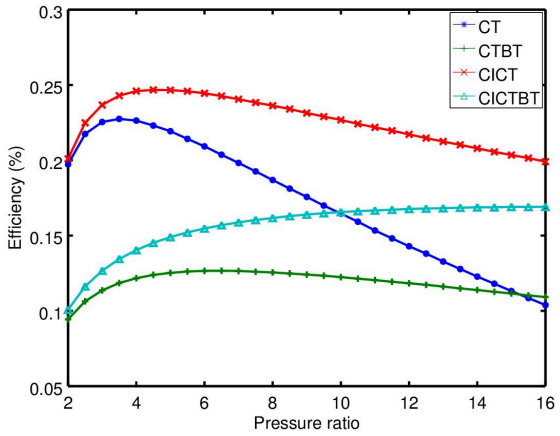

Fig. 4. Fuel conversion efficiency in function of the pressure ratio

The maximum power and efficiency for each configuration, as well as its pressure ratio, are presented in the Table 5. The efficiency maximum occurs in a lower pressure ratio than the power maximum, that behavior is observed for all the configurations, in spite of the maximum were not achieved for CICTBT in the prefixed pressure ratio range (2 to16).

Table 5. Maximum efficiency and power for each configuration.

Configuration	Pressure rate	Efficiency (%)	Pressure rate	Power (kW)
CT	3.5	23.0	5.5	136
CTBT	6.0	12.7	9.5	189
CICT	4.5	24.5	10.0	176
CICTBT	16	16.9	>16	>266

Another way to visualize and easily compare the performance is potting, for each configuration, the efficiency in function of the power, as seen in Fig. 5. Thus, it is noted that the CICT configuration has the best efficiency and obtains significant power. This configuration should be used in a

pressure rate between 4,5 (maximum efficiency) and 10,0 (maximum power). Because of its performance, authors consider that this one is the best configuration option.

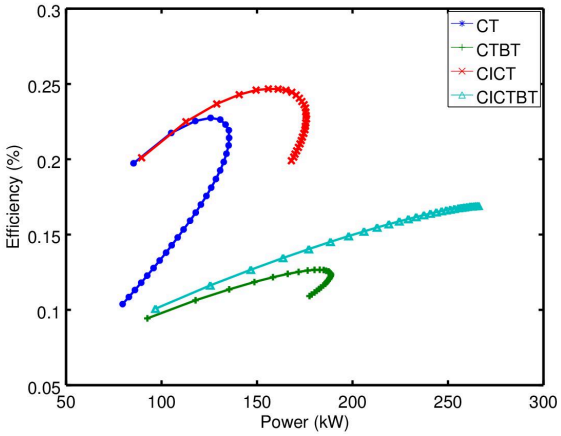

Fig. 5. Fuel conversion efficiency in function of the net power

In terms of heat looses and therefore responsible for the low efficiencies obtained, four different sources are quantified in the model. First of all, the exhaust gases are the main loose source. These gases, that are at least 573K, have associated a heat loose between 2 and 4 times of the net power. As the pressure ratio increase, T_{ch} increase too (see Fig. 6), because of the air-gases heat exchange and considering that T_2 is affected by the pressure ratio. The exhaust gases temperature exceeds 850K for the configuration without intercooler. Both configurations where the compression is made in two steps, the resulting T_2 is lower, and consequently the T_{ch} is lower too.

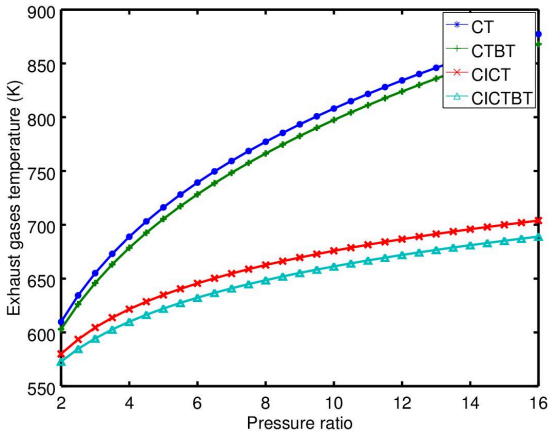

Fig. 6. Exhaust gases temperature in function of the pressure ratio

One way to minimize the looses, and thus increase the efficiency, is employed the EFGT in a combined heat power system (CHP). Considering the high temperature of exhaust gases, this heat has a good quality, which could be used to generate steam or just hot water.

Both configuration that include the compression in two stages have heat looses in the intercooler. They represents between 40% and 100% compared to the net power. These kind of looses are always smaller than the exhaust gases looses. Moreover, the intercooler has to chill the main air flow from T_2 (500-600K) up to T_1 (300K), thus a cool source is needed and the possibility to take advantage of this heat in a CHP can be more difficult.

Lastly, when the expansion is made in two stages and a secondary burner is need, the heat looses of these gases are highly relevant. The burner exhaust temperature, T_{e2}, as been fixed by selected pinch point of 100K above T_4, therefore could achieves values between 1000 and 1200K. Exploit these gases is essential to improve de cycle efficiency.

3.2. Fuel moisture influence

The fuel moisture influence was determined employing eucalyptus wood as a fuel. The chosen pressure ratio was 4.5 in order to get maximum efficiency for CICT configuration. The main air mass flow was 1.0 kg/s and the temperatures T_1 and T_3 were 300K and 1273K respectively.

It should be noted that the net power of the cycle depends just in temperatures and the main air flow. Because of that, the fuel moisture does not affect the power. On the other hand, efficiency and fuel consumption have been affected. When moisture increases, the needs of fuel grows because the adiabatic temperature is attempted to maintain at similar value, with less useful energy by mass of fuel, ensuring T_3 in the heat exchanger outlet for the air flow.

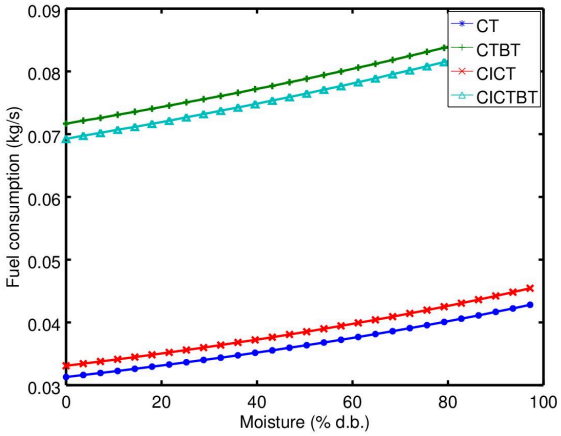

Fig. 7. Fuel consumption in function of the moisture

The Fig. 8 represents the behavior of efficiency when moisture increases. It can be seen that as well as the fuel consumption increase (due to a moisture increase), the efficiency decrease. The efficiency drop reaches 7% between 0% and 100% of moisture in dry basis for the CICT configuration.

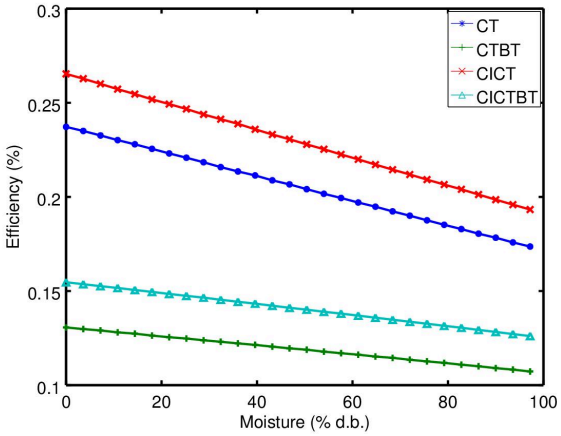

Fig. 8. Fuel conversion efficiency in function of the moisture

Fig. 9 show the dependence of the adiabatic and exhaust gases temperatures, respectably, by the fuel moisture for each EFGT configuration. Noted that the adiabatic temperature has a slight decline when the moisture increases. The reason for that behavior is the fact that with the moisture increase the fuel consumption so increase the gases mass flow and the needed adiabatic temperature to guarantee the heat exchange is lower. However, the exhaust gases temperature is seen increased and the heat looses too.

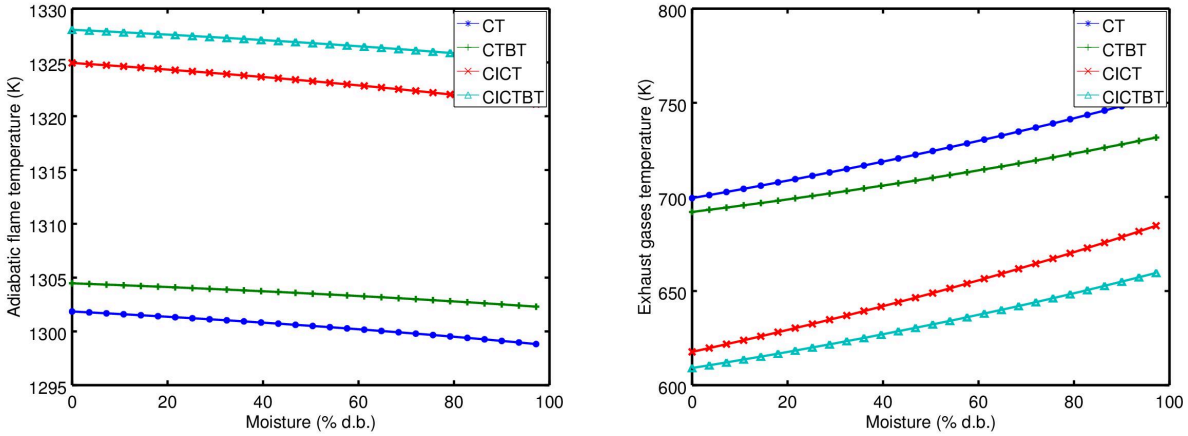

Fig. 9. Adiabatic flame temperature as a function of the moisture (left). Exhaust gases temperature as a function of the moisture(right).

3.3. Biomasses performance

Six biomasses, with different LHV, ash content and elemental compositions, were tested under the same conditions of pressure ratio (4.5), moisture (25% d.b.), T_1 (300K), T_3 (1173K), air mass flow (1.0 kg/s), to evaluate de performance in the for EFGT that are in consideration.

Both, efficiency and fuel consumption of the gas turbine have been affected by the fuel characteristics variations. Other parameters, such as power, adiabatic temperature and exhaust gases temperature have not modifications, or the results oscillation are really small (around 1% or less).

Looking at the fuel characteristics, it was expected that rice husk and eucalyptus bark have the biggest performance variations compared to eucalyptus wood. The efficiency shows a relative drop of 3.5% for the rice husk compared to the eucalyptus wood.

In terms of fuel consumption, due to the high ash content of rice husk (18.9% d.b.) and poor LHV (14800 kJ/kg) compared to eucalyptus wood, the rice husk consumption is about 25% higher than the eucalyptus wood. Eucalyptus bark presents a similar behavior in terms of consumption, where it has to be around 17% over eucalyptus wood. On the other hand, fuels such as pine wood, which has a better LHV, the necessity of fuel is lower compared with eucalyptus (around 6%).

4. Summary and Conclusions

A thermodynamic analysis for a multi-step externally fired gas turbine has been developed. Our model could be used as an a priori global simulation scheme in order to foresee the overall plant efficiency as a function of a reduced set of parameters with a direct thermodynamic meaning. The irreversible thermodynamic cycle model incorporates the possibility of an arbitrary number of turbines N_t and compressors N_c with the associated reheating and intercooling processes and taking account irreversibilities such as pressure drop, non-ideal heat exchangers, and isentropic efficiencies in compressors and turbines.

As main results we stress the following points.

- A CT configuration of EFGT could achieve reasonable values of power and efficiency, with the advantage of an external combustion compared to DFGT.
- Increase the numbers of compressors increases the net power, nevertheless when turbines number is increased, the efficiency decreases drastically. This is because the need of intermediate burner, that implies release exhaust gases at high temperature.
- The use of fuels with higher humidity does not affect the result of the power, however efficiency decreases. That is because the useful energy by mass of fuel, decreases and is needed more fuel to reach the adequate temperature at the inlet turbine.

- Again since the net power of the cycle just depends on temperatures and the main air flow, the change of fuel characteristics not affect their values but, both efficiency and fuel consumption have been affected. The efficiency shows a relative drop of 3.5% for the rice husk compared to the eucalyptus wood. The fuel consumption is increased for those fuels that have higher content of ashes and lower heating values. For fuels studied in the present work the fuel consumption could vary up to 25% related to eucalyptus.

In future works, for configurations of more than two turbines, should be study how to improve the reheating system in order to achieve betters efficiencies. In addition, it is possible to study the potential of this type of engines to work in combined heat and power system, in order to recuperate the heat rejected to the ambient and improve the overall efficiency.

On the other hand the thermodynamic model allows to do an optimizing study in order to identify the main variables that improve the efficiency and get better performance of the system.

Acknowledgments

Alejandro Medina and Antonio Calvo Hernández acknowledges financial support from MINECO (Spain) under grant ENE2013-40644-R. Also P.L Curto-Risso acknowledges support from Universidad de la República and Agencia Nacional de Investigación e Innovación, (Uruguay) for the SNI program that supports his research. A. Durante and G. Pena also acknowledges support from ANII under grant FSE-1-2014-1-102079.

References

[1] COUTO, L.; DIAS MÜLLER, M. Florestas energéticas no Brasil. In: BARBOSA CORTEZ, L. A.; SILVA LORA, E. E.; OLIVARES GÓMEZ, E. Biomassa para energia. Campinas: Unicamp, 2008.

[2] KUATZ, M.; HANSEN, U. The externally-fired gas-turbine (EFGT-Cycle) for decentralized use of biomass, v. 84, p. 795-805, 2007.

[3] AL-ATTAB, K. A.; ZAINAL, Z. A. Biomass Fuel Utilization for Gas Turbine systems. **Universiti Sains Malaysia (USM), School of Mechanical Engineering,** Penang, 2010.

[4] AL-ATTAB, K. A.; ZAINAL, Z. A. Externally fired gas turbine technology: A review. **Applied Energy**, v. 138, n. 474–487, 2015.

[5] AL-ATTAB, K. A.; ZAINAL, Z. A. Performance of high-temperature heat exchangers in biomass fuel powered externally fired gas turbine systems. **Renewable Energy**, v. 35, n. 913–920, 2010.

[6] BATISTA DE MELLO, E.; BORGES MONTEIRO, D. Thermodynamic study of an EFGT (externally fired gas turbine) cycle with one detailed model for the ceramic heat exchanger. **Energy**, v. 45, n. 497-502, 2012.

[7] SÁNCHEZ-ORGAZ, S.; MEDINA, A.; CALVO HERNÁNDEZ, A. Thermodynamic model and optimization of a multi-step irreversible Brayton cycle. **Energy Conversion and Management**, v. 51, p. 2134–2143, 2010.

[8] SÁNCHEZ-ORGAZ, S.; MEDINA, A.; CALVO HERNÁNDEZ, A. Recuperative solar-driven multi-step gas turbine power plants. **Energy Conversion and Management** , v. 67, p. 171–178, 2013.

[9] ROCO, J. M. M. et al. Optimum performance of a regenerative Brayton thermal cycle. **Journal of Applied Physics**, v. 82, p. 2735, 1997.

[10] OLIVENZA-LEÓN, D.; MEDINA, A.; CALVO HERNÁNDEZ, A. Thermodynamic modeling of a hybrid solar gas-turbine power plant. **Energy Conversion and Management**, v. 93, p. 435-447, 2015.

[11] INCROPERA, F. P. et al. **Fundamentals of Heat and Mass Transfer**. 6th. ed. [S.l.]: [s.n.], 2007.

[12] BORBOSA CORTEZ, L. A.; SILVA LORA, E. E.; OLIVARES GÓMEZ, E. **Biomassa para energia**. [S.l.]: Unicamp, 2008.

[13] MEDINA, A. et al. Quasi-Dimensional Simulation of Spark Ignition Engines, From Thermodynamic Optimization to Cyclic Variability. London: Springer, 2014.

[14] LEITNER, J. et al. Estimation of heat capacities of solid mixed oxides. **Thermochimica Acta**, v. 395, p. 27-46, 2003.

[15] PENA VERGARA, G. et al. CHARACTERIZATION AND ENERGY POTENTIAL ASSESSMENT OF. **5th International Conference on Engineering for Waste and Biomass Valorisation**, 25-28 Ausut 2014.